A species' response to spatial climatic variation does not predict its response to climate change

Authors: Daniel L. Perret[1*], Margaret E. K. Evans[2], Dov F. Sax[3,4]

Affiliations:

[1] Oak Ridge Institute for Science and Education, USDA Forest Service

[2] Laboratory of Tree Ring Research, University of Arizona, Tucson AZ

[3] Department of Ecology, Evolution, and Organismal Biology, Brown University, Providence RI

[4] Institute at Brown for Environment and Society, Brown University, Providence RI

[*] Corresponding author: daniel.perret@usda.gov

Abstract: The dominant paradigm for assessing ecological responses to climate change assumes that future states of individuals and populations can be predicted by current, species-wide performance variation across spatial climatic gradients. However, the fates of ecological systems may be better predicted by past responses to in-situ temporal climatic variation. Leveraging ponderosa pine tree-ring time series, we test whether statistically inferred responses to spatial versus temporal climatic variation better predict how trees have responded to recent climate change. Predictions derived from spatial climatic variation are wrong in both the magnitude and the direction of how tree growth has responded to climate change. Future climate scenarios exacerbate this disparity, indicating a need to reconsider the use of spatial climatic variation to accurately predict the ecological impacts of climate change.

One-Sentence Summary: Tree-ring growth records reveal that climate change impacts cannot be predicted by examining how ecological phenomena vary geographically – we need to account for how they have varied through time.

Main Text:

Anthropogenic climate change is impacting nature and the benefits that it provides to humanity, including biodiversity, ecological communities, and ecosystem functions and services (*1*). Documenting and predicting these impacts has been a research priority for decades (*2–4*); however, predicting how climate change may impact specific ecological entities and processes remains challenging. In most cases, predictions of this sort are based upon statistical relationships between some ecological phenomenon and spatial variation in climatic conditions. A particularly prevalent application of this approach involves using species' current geographic occurrence patterns to predict their distribution in the future (*i.e.*, species distribution models, SDMs; *4*, *5*), though it can similarly be used to predict any ecological phenomenon that varies across space (*e.g.*, species' abundance, community composition, a demographic vital rate, ecosystem services). Regardless of the ecological variable of interest, this approach rests upon the assumption that the observed response to spatial climatic variation is predictive of as the response to changing climate through time (*7*). For example, if the individual-level growth rate of a tree increases with temperature across its range, this assumption produces the expectation that growth in all populations will increase as temperatures rise in the future. Similarly, if growth rates are highest in the center of a species' temperature range, the expectation is that future warming will result in growth increases in colder parts of the range, and growth declines in warmer parts of the range (*i.e.*, the "leading edge" and "trailing edge" of a species' distribution; *9*). However, substituting spatial variation for temporal variation in this way is known to be problematic in some cases (*7*, *9–14*) and could be misleading. For example, if populations are tightly adapted to site-specific historic climatic conditions, then increasing temperatures could lead to population declines for each population across the range, and not to leading and trailing range edges. Nevertheless, using spatial variation across species' distributions to make predictions could be justified if errors are small enough that species-wide responses to spatial climatic variation yield informative coarse-scale predictions. Thus, determining the degree of mismatch between predictions based on ecological responses to spatial climatic variation versus in-situ climatic variation through time is critical to establishing the reliability of the currently-dominant method for forecasting biodiversity responses to climate change (*7*, *12*, *13*).

Linking across ecological scales using biogenic time series

Assessing the scope and consequences of these potential mismatches requires data that capture both how an ecological phenomenon varies across spatial climatic gradients (hereafter the *species-wide response*), and how the same phenomenon varies through time in response to *in situ* climatic variation (hereafter the *population-level response*). While most ecological datasets are too limited in either extent or duration to accomplish this, spatial networks of biogenic time series, like the annual growth rings of temperate tree species, provide a rare opportunity (*15*). Tree rings can be used to assess both how quickly a species grows at a given location, as well as how individual performance has varied through time in response to past climatic variation. With time-series data collected from many individuals in many populations across a species' geographic distribution, aggregated population-level responses to temporal climatic variation can be compared to species-wide performance variation across spatial climatic gradients. This makes it possible to determine whether populations have responded to currently changing climatic conditions in a manner consistent with species-wide responses to spatial climatic variation

(scenario *i*, Fig. 1A), or whether populations instead contrast in the slope (scenario *ii*, Fig. 1A) or sign (scenario *iii*, Fig. 1A) of their responses relative to expectations from species-wide patterns.

Here we use ponderosa pine *(Pinus ponderosa* s. l.) (*16*, *17*) in western North America as a case study for comparing species-wide responses to spatial climatic variation against population-level responses to temporal climatic variation. The species and region are particularly well-suited for this: western North America experienced relative climatic stability for much of the 20th century, before a consistent warming trend began in the early 1980s (Fig. 2A). Because high-quality historical climate data are available across the region throughout this period, it is possible to leverage the pre-warming stable period to model trees' responses to both spatial and temporal climatic variation, and compare model predictions to observed responses after secular warming began (Fig. 2A). Individual ponderosa pines typically live 100-1000 years, providing performance time series that span this transition from climatic stability to secular warming. Further, ponderosa pine is a common subject for tree-ring analyses because of the species' clearly-defined annual growth rings and climatic sensitivity (*18*). These climate sensitivities, coupled with the dramatic gradients spanned by the species' highly disjunct geographic distribution (2-17ºC mean annual temperature, 100-2500 mm mean annual precipitation), make ponderosa pine an ideal subject for comparing population-level and species-wide climate responses, and evaluating how differences might influence forecasts of future performance.

We collected tree-ring samples from 23 populations of ponderosa pine, located across much of the species' geographic and climatic distribution in the western United States (Fig. 1C, Table S1; (*19*)). We used standard dendrochronological methods to prepare, crossdate, and measure these samples, and associated annual ring widths with PRISM climate data (see Supplementary Materials & Methods; (*20*)). To quantify both species-wide and population-level climate responses, we used a generalized linear mixed model to predict each tree's annual growth prior to the onset of climate warming (1900-1982) as a function of: *(1)* spatially varying mean climatic conditions, capturing species-wide variation in average growth rate, and *(2)* time-varying climatic variables, capturing aggregated population-level variation in annual growth rates. We also incorporated the effect of individual tree size on growth into the model; see supplementary Methods for further details. We applied this model to ask which statistically inferred response better predicted observed growth following the onset of climate warming (1982-2015), by comparing model-predicted responses to spatial versus temporal climatic variation to observed growth over the same period. Finally, we used a range of CMIP6 future climate scenarios (*21*) to contrast these growth predictions through the end of the 21st century.

Findings

Growth responses to climatic variation differ across space versus through time

The data show that species-wide responses to spatial climatic variation and population-level responses to temporal climatic variation are opposite in sign with respect to temperature but not precipitation. We found evidence of a strong species-wide, positive relationship between mean growth rate and spatial variation in mean temperature and precipitation (Fig. 1B-C), such that trees grew faster in warmer and wetter locations. In contrast, populations show *(1)* a negative relationship between interannual variation in growth rate and temperature, and *(2)* a

weak positive relationship between interannual variation in growth rate and precipitation that is stronger at the driest locations (Fig. 1B-C, Fig. S1). Thus, species-wide versus population-level responses to climate variation are opposite in sign with respect to temperature, consistent with our scenario *iii* (Fig 1A), whereas they contrasted in magnitude with respect to precipitation, consistent with our scenario *ii* (Fig 1A).

Species-wide spatial patterns do not predict growth responses to recent climate change

These contrasting responses resulted in divergent predictions in response to a secular warming trend in the near-past (1982-2015), such that the species-wide response predicted increased growth, whereas population-level responses predicted decreased growth (Fig. 2B, Fig. S2). Comparing these near-past predictions to observed growth trends over the same period showed that population-level responses to interannual climatic variation predicted actual growth trends substantially better than the species-wide response to spatial climatic variation. The performance of predictions based on species-wide patterns declined with the amount of warming a site experienced (r = -0.42, p = 0.04), such that these predictions correlated negatively with observed growth above ~0.5°C of warming (Fig. 2C). This demonstrates that predicting a species' response to climate change based on spatial variation in performance can yield directionally incorrect predictions of how growth may change over a timeframe as short as 40 years. A few recent studies have found similarly contrasting responses to spatial versus temporal environmental variation (*13*, *22–24*), thus implying that this type of space-for-time prediction may be misleading. Here we have directly tested this implication by asking whether responses to spatial climatic variation across a species' distribution accurately predict actual observed responses to changing climate.

Future climate change exacerbates prediction errors

The finding that species-wide patterns fail to predict actual responses on short decadal timescales raises concern about the accuracy of predictions made over the longer timescales that are typically used when forecasting species' responses to climate change, *e.g.*, to the end of the 21st century (*3*). To examine this, we extended our projections of ponderosa pine's performance out to the end of the century (2015-2100) under a range of future CMIP6 climate scenarios (SSP1-2.6, SSP2-4.5, SSP5-8.5;(*21*)). We found that in all future climate scenarios, the responses to spatial versus temporal climatic variation predict dramatically different performance trajectories (Fig. 2D, Fig. S3, Fig. S4). Under the SSP5-8.5 scenario, forecasts based on the response to spatial climatic variation indicated growth increases of up to 300%, compared to projected growth declines in most populations when forecasts were based on the response to interannual climatic variation (Fig. 2D). Notably, across populations, the degree to which the two predictions diverged depended strongly on the amount of future warming projected at the study site with the largest divergences occurring with the greatest projected warming (Fig. 2E, Fig. S3, Fig. S4).

Implications and outlook

Whether population-level predictions based on responses to within-site temporal variation in climate continue to be more accurate than predictions based on the response to spatial climatic variation depends on a variety of processes, including plasticity, evolutionary adaptation, and migration (*8*, *25*, *26*). An emerging body of work has indicated that individual tree growth responses to interannual climate variability may change through time as trees are exposed to different ranges of climatic conditions (*27–30*). Unfortunately, this sort of plasticity is likely to accelerate growth declines as trees experience conditions beyond the range of variability to which they are adapted (*27*, *31*, *32*). Thus, predictions of future tree growth based on static, linear relationships between interannual climatic variation and growth, including our predictions, may be overly optimistic and in fact underestimate future growth declines. Whether transgenerational plasticity could shift climate sensitivities through parental effects on offspring phenotypes is currently unknown (*33*, *34*). However, given increasing climatic variability and the complexity of environmental cues, any such parental effects have a high likelihood of being detrimental rather than helping to compensate for declining performance (*34*). Over longer timescales, evolutionary adaptation to changing conditions could compensate for declining performance, through selection for either higher mean growth rates or different climate sensitivities (*25*, *35*, *36*). However, this evolutionary rescue seems unlikely to result in meaningful change over the time period we examine here, given the rapid pace of climate change relative to the slow demographic rates of long-lived tree species (*36–39*). Adaptive responses to climate change could be accelerated or otherwise facilitated by migration of genotypes better-suited to current and future climatic conditions (*25*, *40*). However, naturally-occurring tree dispersal already lags behind the pace of climate change (*41*) and may be further hindered by human land use, biotic interactions, or other factors that limit range shifts. Thus, while plasticity, adaptation, and migration are important processes in determining species' future trajectories, it is unclear whether they have the capacity to substantially alter the results or implications of the work we present here over the projection timeframe.

This study provides a rare empirical test of whether the impact of recent climate change can be predicted by a species' relationship to spatial climatic variation; we find that it cannot. Further, we demonstrate that an alternative approach leveraging time series data matches observed growth responses to climate change quite well. There are numerous recent examples of studies using spatial patterns to forecast future tree growth and other performance metrics (*e.g.*, *6*, *7*, *43–45*). Our results suggest that this currently prevailing practice will not accurately predict the future growth of ponderosa pine or other trees (*e.g.*, *Pseudotsuga menzeisii; 14*). More broadly, recent corroborative evidence suggests that our findings and their implications may be generally relevant for the practice of ecological forecasting. Several recent studies have described contrasting responses of ecological phenomena to spatial versus temporal environmental variation in a wide variety of contexts [*e.g.*, growth rates of other tree species (*22*, *47*), demographic rates in perennial bunchgrasses (*48*), patterns of pathogen-driven forest mortality (*49*), demographic vital rates of regional bird populations (*23*, *24*, *50*), and in the population growth rates of an endemic alpine plant (*51*)]. The implication of our results is that in the presence of such contrasting responses, predictions based solely on the response to spatial environmental variation can be misleading not just in magnitude, but in sign, *i.e.*, directionally incorrect. This raises concern about the broad application of models that only consider species' responses to spatial variation for forecasting.

A growing body of work has already begun documenting cases where observed responses to climate are at odds with spatially-based predictions (*50–57*). Our results suggest that

contrasting ecological responses across space versus through time could be responsible for these mismatches, though there are undoubtedly more possible causes. To improve ecological forecasting, we believe that there is an urgent need to better understand in which cases *in situ* temporal variation versus spatial variation will produce more accurate forecasts of future ecological states – including not only tree growth, but also species' distributions, ecosystem productivity, and other socially-valuable ecological phenomena. Critically important work aiming to move beyond the current spatially-based paradigm by integrating different sources of information has already been fruitful (*58–60*). Ultimately, improving our ability to make accurate, reliable forecasts will require systematic exploration of mismatches between ecological responses to spatial and temporal climate variability, as well as further development of data, methods, and models for incorporating both sources of variability.

References and Notes

1. IPBES, *Global assessment report of the Intergovernmental Science-Policy Platform on Biodiversity and Ecosystem Services* (2019; https://ipbes.net/global-assessment%0Ahttps://ipbes.net/global-assessment-report-biodiversity-ecosystem-services).
2. C. D. Thomas, A. Cameron, R. E. Green, M. Bakkenes, L. J. Beaumont, Y. C. Collingham, B. F. N. Erasmus, M. F. De Siqueira, A. Grainger, L. Hannah, L. Hughes, B. Huntley, A. S. Van Jaarsveld, G. F. Midgley, L. Miles, M. a Ortega-Huerta, a T. Peterson, O. L. Phillips, S. E. Williams, Extinction risk from climate change. *Nature*. **427**, 145–8 (2004).
3. M. C. Urban, Accelerating extinction risk from climate change. *Science (80-.).* **348**, 571–573 (2015).
4. J. M. Serra-Diaz, J. Franklin, What's hot in conservation biogeography in a changing climate? Going beyond species range dynamics. *Divers. Distrib.* **25**, 492–498 (2019).
5. J. Elith, J. R. Leathwick, Species distribution models: Ecological explanation and prediction across space and time. *Annu. Rev. Ecol. Evol. Syst.* **40**, 677–697 (2009).
6. J. Franklin, Species distribution models in conservation biogeography: Developments and challenges. *Divers. Distrib.* **19**, 1217–1223 (2013).
7. P. B. Adler, E. P. White, M. H. Cortez, Matching the forecast horizon with the relevant spatial and temporal processes and data sources. *Ecography (Cop.).* **43**, 1729–1739 (2020).
8. J. C. Svenning, B. Sandel, Disequilibrium vegetation dynamics under future climate change. *Am. J. Bot.* **100**, 1266–1286 (2013).
9. S. A. Woodin, T. J. Hilbish, B. Helmuth, S. J. Jones, D. S. Wethey, Climate change, species distribution models, and physiological performance metrics: Predicting when biogeographic models are likely to fail. *Ecol. Evol.* **3**, 3334–3346 (2013).
10. K. C. Baer, J. L. Maron, Ecological niche models display nonlinear relationships with abundance and demographic performance across the latitudinal distribution of Astragalus utahensis (Fabaceae). *Ecol. Evol.* **10**, 8251–8264 (2020).
11. G. Midolo, C. Wellstein, S. Faurby, Individual fitness is decoupled from coarse-scale probability of occurrence in North American trees. *Ecography (Cop.).* **44**, 789–801 (2021).
12. A. J. Felton, R. K. Shriver, M. Stemkovski, J. B. Bradford, K. N. Suding, P. B. Adler, Climate disequilibrium dominates uncertainty in long-term projections of primary productivity. *Ecol. Lett.* **25**, 2688–2698 (2022).
13. S. Klesse, R. J. DeRose, F. Babst, B. A. Black, L. D. L. Anderegg, J. Axelson, A. Ettinger, H. Griesbauer, C. H. Guiterman, G. Harley, J. E. Harvey, Y. H. Lo, A. M. Lynch, C. O'Connor, C. Restaino, D. Sauchyn, J. D. Shaw, D. J. Smith, L. Wood, J. Villanueva-Díaz, M. E. K. Evans, Continental-scale tree-ring-based projection of Douglas-fir growth: Testing the limits of space-for-time substitution. *Glob. Chang. Biol.* **26**, 5146–5163 (2020).
14. M. Isaac-Renton, D. Montwé, A. Hamann, H. Spiecker, P. Cherubini, K. Treydte, Northern forest tree populations are physiologically maladapted to drought. *Nat. Commun.* **9**, 1–9 (2018).
15. M. E. K. Evans, B. A. Black, D. A. Falk, C. L. Giebink, E. L. Schultz, in *Demographic Methods Across the Tree of Life* (Oxford University Press, 2021), p. 77.
16. A. Willyard, D. S. Gernandt, K. Potter, V. Hipkins, P. Marquardt, M. F. Mahalovich, S. K.

Langer, F. W. Telewski, B. Cooper, C. Douglas, K. Finch, H. H. Karemera, J. Lefler, P. Lea, A. Wofford, Pinus ponderosa: A checkered past obscured four species. *Am. J. Bot.* **104**, 161–181 (2017).

17. A. Willyard, D. S. Gernandt, A. López-Reyes, K. M. Potter, Mitochondrial phylogeography of the ponderosa pines: widespread gene capture, interspecific sharing, and two unique lineages. *Tree Genet. Genomes*. **17**, 1–19 (2021).
18. I. M. McCullough, F. W. Davis, A. P. Williams, A range of possibilities: Assessing geographic variation in climate sensitivity of ponderosa pine using tree rings. *For. Ecol. Manage.* **402**, 223–233 (2017).
19. D. L. Perret, D. F. Sax, Evaluating alternative study designs for optimal sampling of species' climatic niches. *Ecography (Cop.).*, 1–12 (2021).
20. C. Daly, M. Halbleib, J. I. Smith, W. P. Gibson, M. K. Doggett, G. H. Taylor, J. Curtis, P. P. Pasteris, Physiographically sensitive mapping of climatological temperature and precipitation across the conterminous United States. *Int. J. Climatol.* **28**, 2031–2064 (2008).
21. V. Eyring, S. Bony, G. A. Meehl, C. A. Senior, B. Stevens, R. J. Stouffer, K. E. Taylor, Overview of the Coupled Model Intercomparison Project Phase 6 (CMIP6) experimental design and organization. *Geosci. Model Dev.* **9**, 1937–1958 (2016).
22. C. D. Canham, L. Murphy, R. Riemann, R. McCullough, E. Burrill, Local differentiation in tree growth responses to climate. *Ecosphere*. **9**, e02368 (2018).
23. P. Gaüzère, V. Devictor, Mismatches between birds' spatial and temporal dynamics reflect their delayed response to global changes. *Oikos*. **130**, 1284–1296 (2021).
24. F. A. La Sorte, M. L. Tien, H. Wilman, W. Jetz, Disparities between observed and predicted impacts of climate change on winter bird assemblages. *Proc. R. Soc. B Biol. Sci.* **276**, 3167–3174 (2009).
25. S. N. Aitken, S. Yeaman, J. A. Holliday, T. Wang, S. Curtis-McLane, Adaptation, migration or extirpation: climate change outcomes for tree populations. *Evol. Appl.* **1**, 95–111 (2008).
26. F. Valladares, S. Matesanz, F. Guilhaumon, M. B. Araújo, L. Balaguer, M. Benito-Garzón, W. Cornwell, E. Gianoli, M. van Kleunen, D. E. Naya, A. B. Nicotra, H. Poorter, M. A. Zavala, The effects of phenotypic plasticity and local adaptation on forecasts of species range shifts under climate change. *Ecol. Lett.* **17**, 1351–1364 (2014).
27. J. Astigarraga, E. Andivia, M. A. Zavala, A. Gazol, V. Cruz-Alonso, S. M. Vicente-Serrano, P. Ruiz-Benito, Evidence of non-stationary relationships between climate and forest responses: Increased sensitivity to climate change in Iberian forests. *Glob. Chang. Biol.* **26**, 5063–5076 (2020).
28. D. M. P. Peltier, K. Ogle, Tree growth sensitivity to climate is temporally variable. *Ecol. Lett.* **23**, 1561–1572 (2020).
29. M. Wilmking, M. van der Maaten-Theunissen, E. van der Maaten, T. Scharnweber, A. Buras, C. Biermann, M. Gurskaya, M. Hallinger, J. Lange, R. Shetti, M. Smiljanic, M. Trouillier, Global assessment of relationships between climate and tree growth. *Glob. Chang. Biol.* **26**, 3212–3220 (2020).
30. R. M. Keen, S. L. Voelker, S. -Y. S. Wang, B. J. Bentz, M. Goulden, C. R. Dangerfield, C. C. Reed, S. M. Hood, A. Z. Csank, T. E. Dawson, A. G. Merschel, C. J. Still, Changes in tree drought sensitivity provided early warning signals to the California drought and forest mortality event. *Glob. Chang. Biol.*, 1–14 (2021).
31. F. Babst, O. Bouriaud, B. Poulter, V. Trouet, M. P. Girardin, D. C. Frank, Twentieth century redistribution in climatic drivers of global tree growth. *Sci. Adv.* **5**, 1–10 (2019).

32. M. P. Dannenberg, E. K. Wise, W. K. Smith, Reduced tree growth in the semiarid United States due to asymmetric responses to intensifying precipitation extremes. *Sci. Adv.* **5**, 1–11 (2019).
33. E. A. Harmon, D. W. Pfennig, Evolutionary rescue via transgenerational plasticity: Evidence and implications for conservation. *Evol. Dev.* **23**, 292–307 (2021).
34. S. C. Donelan, J. K. Hellmann, A. M. Bell, B. Luttbeg, J. L. Orrock, M. J. Sheriff, A. Sih, Transgenerational Plasticity in Human-Altered Environments. *Trends Ecol. Evol.* **35**, 115–124 (2020).
35. J. R. Etterson, R. G. Shaw, Constraint to adaptive evolution in response to global warming. *Science (80-.).* **294**, 151–154 (2001).
36. A. A. Hoffmann, C. M. Sgró, Climate change and evolutionary adaptation. *Nature*. **470**, 479–485 (2011).
37. C. Moritz, R. Agudo, The future of species under climate change: Resilience or decline? *Science (80-.).* **341**, 504–508 (2013).
38. S. Lavergne, N. Mouquet, W. Thuiller, O. Ronce, Biodiversity and climate change: Integrating evolutionary and ecological responses of species and communities. *Annu. Rev. Ecol. Evol. Syst.* **41**, 321–350 (2010).
39. F. J. Alberto, S. N. Aitken, R. Alía, S. C. González-Martínez, H. Hänninen, A. Kremer, F. Lefèvre, T. Lenormand, S. Yeaman, R. Whetten, O. Savolainen, Potential for evolutionary responses to climate change - evidence from tree populations. *Glob. Chang. Biol.* **19**, 1645–1661 (2013).
40. G. A. O'neill, E. Gómez-Pineda, Local was best: Sourcing tree seed for future climates. *Can. J. For. Res.* **51**, 1432–1439 (2021).
41. K. Zhu, C. W. Woodall, J. S. Clark, Failure to migrate: Lack of tree range expansion in response to climate change. *Glob. Chang. Biol.* **18**, 1042–1052 (2012).
42. A. R. Weiskittel, N. L. Crookston, P. J. Radtke, Linking climate, gross primary productivity, and site index across forests of the western United States. *Can. J. For. Res.* **41**, 1710–1721 (2011).
43. N. M. Tchebakova, E. I. Parfenova, M. A. Korets, S. G. Conard, Potential change in forest types and stand heights in central Siberia in a warming climate. *Environ. Res. Lett.* **11** (2016), doi:10.1088/1748-9326/11/3/035016.
44. H. Jiang, P. J. Radtke, A. R. Weiskittel, J. W. Coulston, P. J. Guertin, Climate- and soil-based models of site productivity in eastern US tree species. *Can. J. For. Res.* **45**, 325–342 (2015).
45. A. R. Weiskittel, N. L. Crookston, G. E. Rehfeldt, Projected future suitable habitat and productivity of Douglas-fir in western North America. *Schweizerische Zeitschrift fur Forstwes.* **163**, 70–78 (2012).
46. C. Andrews, J. R. Foster, A. Weiskittel, A. W. D'Amato, E. Simons-Legaard, Integrating historical observations alters projections of eastern North American spruce–fir habitat under climate change. *Ecosphere*. **13**, 1–14 (2022).
47. S. Klesse, R.J. DeRose, F.Babst, B. Black, L.D.L. Anderegg, J. Axelson, A. Ettinger, H. Griesbauer, C.H. Guiterman, G. Harley, J.E. Harvey, Y.H. Lo, A.M. Lynch, C. O'Connor, C. Restaino, D. Sauchyn, J. Shaw, D. Smith, L. Wood, J. Villanueva, M.E.K. Evans, Continental-scale tree-ring based projection of Douglas-fir growth – Testing the limits of space- for-time substitution. *Glob. Chang. Biol.*, 0–3 (2020).
48. M. L. Peterson, G. Bailes, L. B. Hendricks, L. Pfeifer-Meister, P. B. Reed, S. D. Bridgham, B. R. Johnson, R. Shriver, E. Waddle, H. Wroton, D. F. Doak, B. A. Roy, W. F. Morris, Latitudinal gradients in population growth do not reflect demographic

responses to climate. *Ecol. Appl.* **31**, 1–13 (2021).

49. B. J. Harvey, R. A. Andrus, M. A. Battaglia, J. F. Negrón, A. Orrego, T. T. Veblen, Droughty times in mesic places: factors associated with forest mortality vary by scale in a temperate subalpine region. *Ecosphere*. **12** (2021), doi:10.1002/ecs2.3318.
50. S. Bonthoux, J. Y. Barnagaud, M. Goulard, G. Balent, Contrasting spatial and temporal responses of bird communities to landscape changes. *Oecologia*. **172**, 563–574 (2013).
51. M. F. Oldfather, M. J. Koontz, D. F. Doak, D. D. Ackerly, Range dynamics mediated by compensatory life stage responses to experimental climate manipulations. *Ecol. Lett.* **24**, 772–780 (2021).
52. C. M. Beale, J. J. Lennon, A. Gimona, Opening the climate envelope reveals no macroscale associations with climate in European birds. *Proc. Natl. Acad. Sci. U. S. A.* **105**, 14908–14912 (2008).
53. B. J. McGill, Trees are rarely most abundant where they grow best. *J. Plant Ecol.* **5**, 46–51 (2012).
54. N. I. Chardon, S. Pironon, M. L. Peterson, D. F. Doak, Incorporating intraspecific variation into species distribution models improves distribution predictions, but cannot predict species traits for a wide-spread plant species. *Ecography (Cop.).* **43**, 60–74 (2020).
55. T. A. Dallas, A. Hastings, Habitat suitability estimated by niche models is largely unrelated to species abundance. *Glob. Ecol. Biogeogr.* **27**, 1448–1456 (2018).
56. L. Santini, S. Pironon, L. Maiorano, W. Thuiller, Addressing common pitfalls does not provide more support to geographical and ecological abundant-centre hypotheses. *Ecography (Cop.).* **42**, 696–705 (2019).
57. A. Jiménez-Valverde, P. Aragón, J. M. Lobo, Deconstructing the abundance–suitability relationship in species distribution modelling. *Glob. Ecol. Biogeogr.* **30**, 327–338 (2021).
58. N. J. Briscoe, J. Elith, R. Salguero-Gómez, J. J. Lahoz-Monfort, J. S. Camac, K. M. Giljohann, M. H. Holden, B. A. Hradsky, M. R. Kearney, S. M. McMahon, B. L. Phillips, T. J. Regan, J. R. Rhodes, P. A. Vesk, B. A. Wintle, J. D. L. Yen, G. Guillera-Arroita, Forecasting species range dynamics with process-explicit models: matching methods to applications. *Ecol. Lett.* **22**, 1940–1956 (2019).
59. M. C. Urban, G. Bocedi, A. P. Hendry, J. B. Mihoub, G. Pe'er, A. Singer, J. R. Bridle, L. G. Crozier, L. De Meester, W. Godsoe, A. Gonzalez, J. J. Hellmann, R. D. Holt, A. Huth, K. Johst, C. B. Krug, P. W. Leadley, S. C. F. Palmer, J. H. Pantel, A. Schmitz, P. A. Zollner, J. M. J. Travis, Improving the forecast for biodiversity under climate change. *Science (80-.).* **353** (2016), doi:10.1126/science.aad8466.
60. D. Zurell, W. Thuiller, J. Pagel, J. S. Cabral, T. Münkemüller, D. Gravel, S. Dullinger, S. Normand, K. H. Schiffers, K. A. Moore, N. E. Zimmermann, Benchmarking novel approaches for modelling species range dynamics. *Glob. Chang. Biol.* **22**, 2651–2664 (2016).
61. A. Farjon, D. Filer, *An Atlas of the World's Conifers* (Koninklijke Brill, Leiden, The Netherlands, 2013).
62. K. C. Maguire, D. J. Shinneman, K. M. Potter, V. D. Hipkins, Intraspecific niche models for ponderosa pine (Pinus ponderosa) suggest potential variability in population-level response to climate change. *Syst. Biol.* **2892** (2018), doi:10.1093/sysbio/syy017/4934308.
63. A. Farjon, The Conifer Database (2021), (available at https://herbaria.plants.ox.ac.uk/bol/conifers).
64. D. L. Perret, A. B. Leslie, D. F. Sax, Naturalized distributions show that climatic disequilibrium is structured by niche size in pines (Pinus L .). *Glob. Ecol. Biogeogr.* **28**, 429–441 (2019).

65. V. C. Lessard, T. D. Drummer, D. D. Reed, Precision of density estimates from fixed-radius plots compared to n-tree distance sampling. *For. Sci.* **48**, 1–6 (2002).
66. J. H. Speer, *Fundamentals of Tree-Ring Research* (University of Arizona Press, Tucson, 2012).
67. Cybis, CooRecorder (2021), (available at https://www.cybis.se/forfun/dendro/).
68. Cybis, CDendro (2021) (available at https://www.cybis.se/forfun/dendro/).
69. A. G. Bunn, A dendrochronology program library in R (dplR). *Dendrochronologia*. **26**, 115–124 (2008).
70. A. G. Bunn, Statistical and visual crossdating in R using the dplR library. *Dendrochronologia*. **28**, 251–258 (2010).
71. R. L. Phipps, Some geometric constraints on ring-width trend. *Tree-Ring Res.* **61**, 73–76 (2005).
72. S. Klesse, R. J. Derose, C. H. Guiterman, A. M. Lynch, C. D. O. Connor, J. D. Shaw, M. E. K. Evans, Sampling bias overestimates climate change impacts on forest growth in the southwestern United States. *Nat. Commun.*, 1–9 (2018).
73. K. A. Heilman, M. C. Dietze, A. A. Arizpe, J. Aragon, A. Gray, J. D. Shaw, A. O. Finley, S. Klesse, R. J. DeRose, M. E. K. Evans, Ecological forecasting of tree growth: Regional fusion of tree-ring and forest inventory data to quantify drivers and characterize uncertainty. *Glob. Chang. Biol.*, 1–19 (2022).
74. C. M. Restaino, D. L. Peterson, J. Littell, Increased water deficit decreases Douglas fir growth throughout western US forests. *Proc. Natl. Acad. Sci.* **113**, 9557–9562 (2016).
75. C. E. Littlefield, S. Z. Dobrowski, J. T. Abatzoglou, S. A. Parks, K. T. Davis, A climatic dipole drives short- and long-term patterns of postfire forest recovery in the western United States, 1–8 (2020).
76. W. R. Skinner, J. A. Majorowicz, Regional climatic warming and associated twentieth century land-cover changes in north-western North America. *Clim. Res.* **12**, 39–52 (1999).
77. S. Z. Dobrowski, J. Abatzoglou, A. K. Swanson, J. A. Greenberg, A. R. Mynsberge, Z. A. Holden, M. K. Schwartz, The climate velocity of the contiguous United States during the 20th century. *Glob. Chang. Biol.* **19**, 241–251 (2013).
78. J. T. Abatzoglou, A. P. Williams, Impact of anthropogenic climate change on wildfire across western US forests. *Proc. Natl. Acad. Sci. U. S. A.* **113**, 11770–11775 (2016).
79. J. T. Abatzoglou, S. Z. Dobrowski, S. A. Parks, Multivariate climate departures have outpaced univariate changes across global lands. *Sci. Rep.* **10**, 1–9 (2020).
80. V. M. R. Muggeo, Interval estimation for the breakpoint in segmented regression: a smoothed score-based approach. *Aust. New Zeal. J. Stat.* **59**, 311–322 (2017).
81. P. C. Bürkner, Advanced Bayesian multilevel modeling with the R package brms. *R J.* **10**, 395–411 (2018).
82. T. Wang, A. Hamann, D. Spittlehouse, C. Carroll, Locally downscaled and spatially customizable climate data for historical and future periods for North America. *PLoS One*. **11**, 1–17 (2016).

Acknowledgments: We extend our gratitude to Sharmila Dey, Courtney Giebink, Kelly Heilman, Stephen Jackson, Andrew Leslie, Jon Witman, and Harold Zald for insightful discussion about this work; and to Molly McDevitt for fieldwork assistance. MEKE additionally acknowledges the important influence of past collaboration with Stefan Klesse on her contribution to this work. We thank the following for permitting sample collection: Apache-Sitgreaves, Arapaho and Roosevelt, Mendocino, Shasta-Trinity, Stanislaus, Mendocino, Wasatch-Cache, and White River National Forests; Regions 1 and 6 of the United States Forest Service; Boulder County Parks and Open Space; and the US Bureau of Land Management.

Funding:
Brown University Department of Ecology, Evolution, and Organismal Biology (DLP)
Institute at Brown for Environment and Society (DLP)
American Philosophical Society Lewis & Clark Fund for Exploration and Field Research (DLP)
U.S. National Science Foundation award MSB-ECA 1802893 (MEKE)

Author contributions:

Conceptualization: DLP, MEKE, DFS

Methodology: DLP, MEKE, DFS

Resources: DLP, DFS

Investigation: DLP

Data Curation: DLP

Formal Analysis: DLP

Supervision: MEKE, DFS

Writing – original draft: DLP

Writing – review & editing: DLP, MEKE, DFS

Competing interests: Authors declare they have no competing interests.

Data and materials availability: All data and code necessary to replicate results are stored at the corresponding author's GitHub repository: https://github.com/daniel-perret/PIPO_treerings

Supplementary Materials:

Materials and Methods

Figs. S1 to S6

Table S1

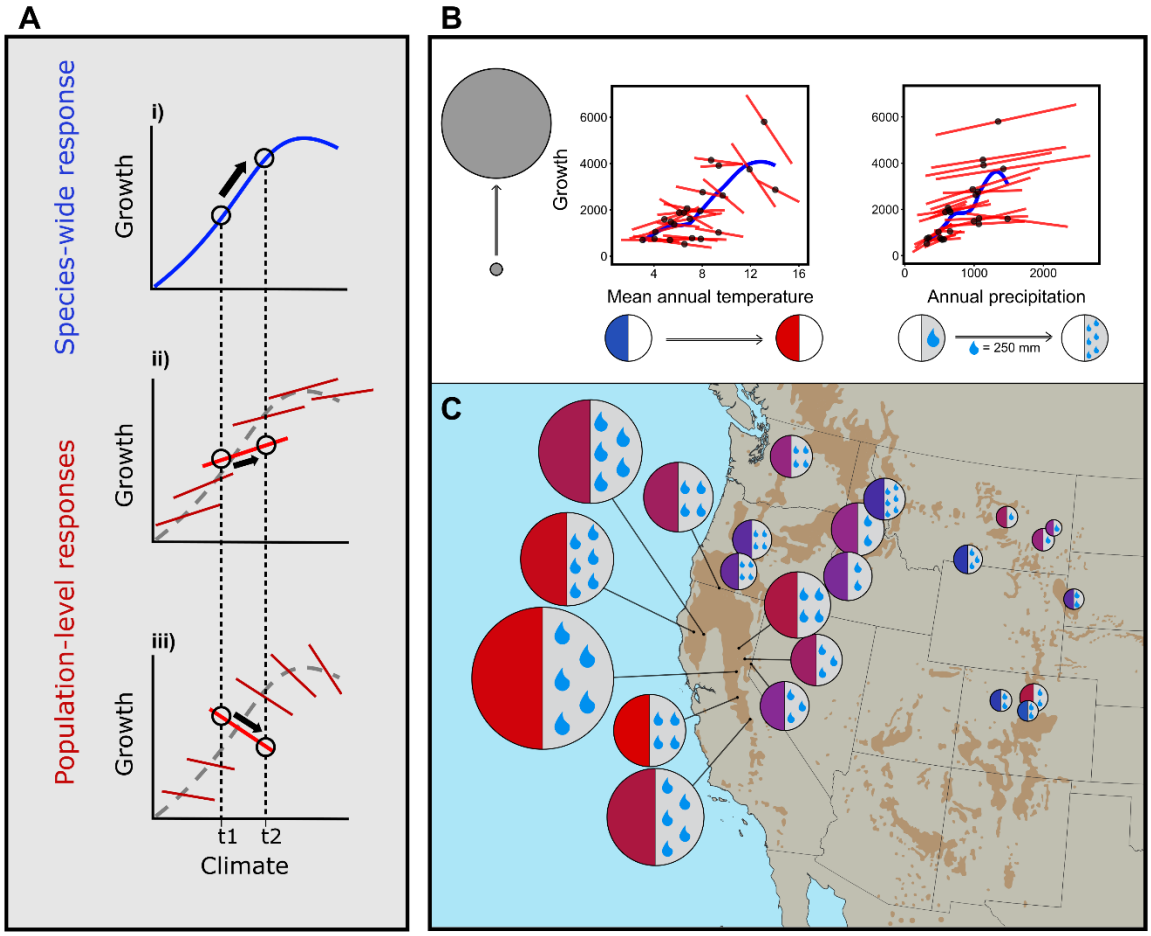

Figure 1. Contrasting responses to spatial versus temporal climatic variation result in dramatically different predictions of future growth. (**A)** Three scenarios of how species-wide responses to spatial climatic variation (blue line, gray dashed lines) could differ from responses of populations to interannual climatic variation (red lines): (*i*) *matching responses*, in which species-wide and population-level responses are identical; *(ii) mismatched slopes*, in which responses differ in their strength, but match in sign; and *(iii) mismatched signs*, in which species-wide and population-level responses are directionally opposed. When climate changes from t_1 to t_2, each scenario yields different predicted growth responses. **(B)** Observed climate-growth relationships across 23 ponderosa pine (*Pinus ponderosa s.l.*) populations. Black points indicate long-term mean climate and growth for each study site; blue lines are locally-weighted regressions illustrating the species-wide spatial climate-growth relationship. Each red line indicates the linear relationship between interannual climatic variation and growth within a single population. **(C)** Study sites were distributed across the geographic and climatic distribution of ponderosa pine, spanning gradients in mean growth rate (size of circle) and average climatic conditions, indicated inside each circle (see axis legends, panel B).

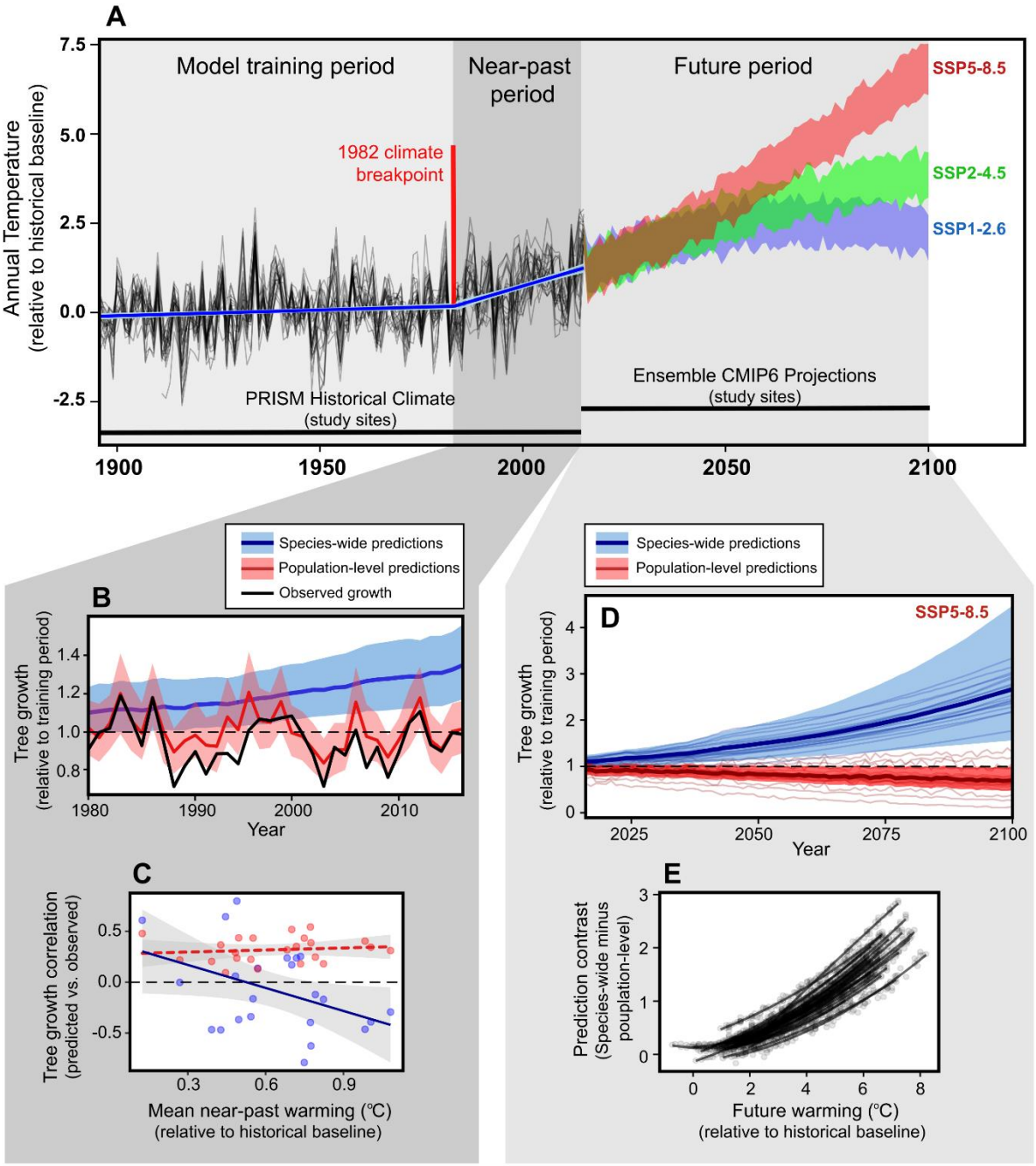

Figure 2. Population-level climate responses better predicted observed growth trends during the near-past period of climate change, and yield forecasts that diverge substantially from those generated using the species-wide response. (A) Mean annual temperature anomalies (°C) at each of our 23 study sites relative to 1900-1950 historical baselines, based on PRISM historical climate data (black lines) and three CMIP6 future climate scenarios (SSP1-2.6, blue; SSP2-4.5, green; SSP5-8.5, red). A breakpoint regression analysis (blue line) of these historical climate time series found a significant breakpoint in 1982, used to define the boundary between model training and near-past prediction time periods. **(B)** Mean

posterior growth predictions and 95% credible intervals during the near-past period, for species-wide predictions (blue) and population-specific predictions (red), compared to observed growth during the same period (black line), averaged across all study sites. Supplementary materials contain predictions for each site. **(C)** Correlations between predicted and observed growth (Pearson's *r*), in relation to mean warming recorded at each site over the near-past period. **(D)** Divergence between species-wide (blue) and population-level (red) growth predictions under the SSP5-8.5 scenario. Heavy lines and shading indicate mean posterior predictions and 95% credible intervals across all sites, respectively; light lines indicate mean posterior predictions for each site. **(E)** Contrasts between species-wide and population-level predictions, as a function of projected future warming at each site (black points and lines).

Science
AAAS

Supplementary Materials for

A species' response to spatial climatic variation does not predict its response to climate change

Daniel L. Perret, Margaret E. K. Evans, Dov F. Sax
Corresponding author: daniel.perret@usda.gov

The PDF file includes:

Materials and Methods

Study species

Ponderosa pine (*Pinus ponderosa sensu lato*) is widely distributed in western North America throughout a highly disjunct range that encompasses a tremendous breadth of climatic conditions, with mean annual temperatures ranging from 0 to 15 degrees Celsius and 200 to 2100 millimeters of mean annual cumulative precipitation (Figure 1).The most commonly used taxonomy recognizes two varieties of *P. ponderosa*, var. *scopulorum* and var. *ponderosa* – the Pacific and Rocky Mountain varieties, respectively (*61*). The most recent molecular work has found evidence of more complex taxonomic structuring within ponderosa pine (*16*, *17*), indicating at least four lineages that are more distantly related to each other than they are to other species in *Pinus* subsection *Ponderosae*. However, these taxonomic divisions do not align with differences in climate sensitivities (*18*, *62*). The analyses we present here thus treat the species as a single unit, but may alternatively be considered an analysis of population-level variation across a paraphyletic sample of three or four species in subsection *Ponderosae* (*P. benthamiana*, *P. ponderosa*, *P. scopulorum*, and possibly *P. brachyptera; 16*, *17*).

Tree-ring data

Data collection

We selected study populations from across the distribution of ponderosa pine, following the niche-based methodology proposed by Perret & Sax (2021; (*19*)). We used curated and taxonomically verified botanical records compiled in the Conifer Database (*63*) to bound the climate space occupied by ponderosa pine across its geographic distribution. This climate space was defined by a set of seven climatic variables previously used to model the climatic niches of pines and other conifer species (*19*, *64*). We limited site selection to public lands managed by the United States Forest Service or the Bureau of Land Management. Further criteria were that sites were free of obvious recent disturbance (*e.g.,* timber harvest, thinning or other stand management, recent fire), were a minimum of one kilometer from high-traffic roadways, and were not located on either particularly steep slopes or along drainages. Wherever possible, we selected sites such that they corresponded with one of the Conifer Database botanical records used to build the species' climatic niche model. This site selection procedure resulted in 24 study sites, spread across the states of Arizona, California, Colorado, Idaho, Montana, Oregon, and Montana (Figure 1, Table S1).

We used a consistent plot- and survey-based approach to collect tree-ring samples at each study site. Specifically, we established a 25-m by 25-m square plot in a representative portion of the stand at each site. Within this plot, we measured each ponderosa pine's bole diameter at 1.4 m above ground level (*i.e.,* diameter at breast height, DBH) , assessed its condition, recorded the presence or absence of new cones, and recorded any evidence of pathogens (*e.g.,* sap flows, needle blight). Using a Haglöf increment borer, we collected two 4.3 mm-diameter cores from each tree greater than 15 cm DBH in the plot. One core was collected at breast height (140 cm), and the other was collected as close to the ground as possible given available equipment and the individual tree's setting. In cases where there were fewer than 15 suitable trees on a plot, we sampled additional trees at increasing distances from the plot center. For 10 sites, we could not establish a fixed plot due either to excessive understory growth or site terrain characteristics. For these sites, trees were sampled at increasing distances from the intended plot location (*i.e.*, an n-tree sampling design; *66*). Sampling was conducted during the 2018 growing season between June and October.

Sample preparation

All increment cores were mounted, sanded, and visually cross-dated according to standard dendrochronological methods (*66*). We then measured the width in millimeters of each growth ring in every core sample using 2400 dpi digital scans and the computer program CooRecorder (*67*). We verified year assignments of the measured tree ring series using CDendro (*68*) and the 'dplR' package in R 3.6.3 (*69*, *70*). Specifically, we used 20-year lagged inter-series correlations to identify dating and measurement errors across all series per site. These errors were iteratively identified and corrected until all inter-series correlations were above 0.60. Both core samples for each tree were used during visual and statistical cross-dating, but only samples extracted from breast height were retained for growth analyses. For one site, located outside of Show Low, Arizona, a high rate of missing and false rings prevented confident assignment of a year of formation to growth rings. This site was excluded from all subsequent analyses. We used field-measured DBH for each tree to convert these ring width timeseries to annual basal area increments (BAI), a procedure that controls for the influence of increasing tree bole diameter on annual ring widths (*71*). In total, this yielded 360 tree growth time series from 23 sites (Table S1).

Analyses

Climate data

We associated BAI time series for each tree at each site with PRISM LT81m historical monthly climate time series spanning the years 1900 – 2015 (*20*). For each year, we summarized monthly climate data into eight seasonal periods spanning the growing season of the previous year through the end of the current year. In each of these seasons, we calculated mean maximum monthly temperature and cumulative precipitation. To characterize the general climatic regimes at each site, we calculated mean annual temperature and mean annual cumulative precipitation in 30-year moving windows, as well as across the length of the entire time series. These climatic variables are similar to those used in growth analyses for ponderosa pine and other species (*13*, *18*, *72*, *73*). Exploratory analyses indicated that interannual growth was more strongly correlated with these seasonal climatic variables than annual climatic variables. Some analyses have also included composite measures of moisture availability like vapor pressure deficit (*e.g.*, *18*, *75*) or climatic moisture deficit (*e.g.*, *76*), usually derived from a combination of temperature and precipitation measurements. Though these composite variables can be quite informative, we opted to include only mean and maximum temperatures and cumulative precipitation to limit model complexity and ease interpretation.

Substantial climate change has already been reported across western North America over the past several decades (*76–79*). In order to identify when warming began in the climate time series at each of our study sites, we used a breakpoint regression analysis to assess how secular trends in annual temperature anomalies relative to 1900-1950 means have changed across the full time series (1900-2015). Breakpoints identified by this analysis were used to divide growth and climate time series into "pre-warming" and "post-warming" periods in subsequent analyses. These analyses were conducted using the 'segmented' package in R3.6.3 (*80*).

Growth model

We were interested in describing two aspects of growth variation in our dataset: *(1)* species-wide variation in average growth rate associated with spatially varying climate normals, and *(2)* population-specific variation in annual growth associated with time-varying climatic variables. In order to do this, we used a hierarchical generalized linear mixed model implemented in a Bayesian framework to model annual BAI during the pre-warming period as a function of a tree's size in the preceding year, spatially varying climate normals, and time-varying seasonal climate variables:

(1)

$$\mathrm{BAI}_{t,s,y} \sim \beta_0 + \gamma_{0,t,s} + \beta_1 BA_{t,s,y-1} + \gamma_{1,s} BA_{t,s,y-1} + \beta_{2i} CN_{i,s} + \beta_{3j} TA_{j,s,y} + \gamma_{2j,s} TA_{j,s,y} + \beta_{4j} PA_{j,s,y} + \gamma_{3j,s} PA_{j,s,y} + \varepsilon$$

In this model, the BAI in year *y* of tree *t* at site *s* is modeled as the linear combination of that tree's basal area (*BA*) in the previous year, *y-1*, climate normals (*CN*) that vary between sites *s*, and annual climate variables (*TA*, *PA*) that vary across years *y* and sites *s*. Beta terms (**β**) indicate estimated fixed effects describing species-wide responses, whereas gamma (**γ**) terms indicate random effects varying across sites *s* or trees *t*. Hence, $\boldsymbol{\beta_0}$ is the species-wide intercept (average BAI), whereas $\boldsymbol{\gamma_{0,t,s}}$ is a random modification of the species-wide intercept for each tree *t* nested in each site *s*. This random intercept modification accounts for growth variation between sites and between trees within a site caused by non-climatic factors like soil characteristics, topography, stand density, and disturbance histories. Basal area (*BA*) was back-calculated for each tree in every year using the field-measured DBH and ring width time series data, then standardized relative to the mean tree size at each site. Because the influence of tree size on BAI can vary widely, we included a site-level random slope modifier on this term ($\boldsymbol{\gamma_{1,s}}$). The index *i* varies from one to three, denoting one of two climate normal variables *CN*, mean annual temperature and mean annual precipitation, as well as their interaction. The $\boldsymbol{\beta_{2i}}$ coefficients then capture the species-wide relationship between mean climatic conditions and BAI. The index *j* indicates one of eight seasonal periods ranging from the previous year's growing season through the end of the current growing season in year *y*. Thus, the parameters $\boldsymbol{\beta_{3j}}$ and $\boldsymbol{\beta_{4j}}$ describe the fixed species-wide effect of mean monthly maximum temperatures (*TA*) and cumulative precipitation (*PA*), respectively, during each period *j*. The parameters $\boldsymbol{\gamma_{2j,s}}$ and $\boldsymbol{\gamma_{3j,s}}$ capture population-specific deviations from the species-level response to each of the same seasonal predictors. Because growth increments are always greater than zero, with a variance proportional to the mean, we used a Gamma distribution with a logarithmic link function and an estimated dispersion parameter *q* to describe the model error distribution. To accommodate this link function, we added the minimum observed ring width in each series to any missing rings in that series (*i.e.*, years that were identified via cross-dating when no wood formation occurred in the sample).

Past work has indicated that population-specific growth sensitivities to interannual climatic variation vary predictably with the mean temperature and precipitation conditions at a site (*13*, *18*). Because we were interested in estimating both species-wide and population-level climate responses, we accounted for population-specific variation in climate sensitivities by adding in the site-level random slope modifiers $\boldsymbol{\gamma_{2j,s}}$ and $\boldsymbol{\gamma_{3j,s}}$. In addition, recent work has questioned the assumption of stationarity in climate responses through time that underlies a substantial portion of the dendrochronological literature (*27–30*). Because this work indicates that the climate sensitivities of a single tree can change through time as climate changes, we fit our model using only climate and growth data from the pre-warming period identified in our exploratory analyses of climate time series.

The high dimensionality of these random effects ($\boldsymbol{\gamma}$ terms) in our growth model made it difficult to obtain stable coefficient estimates using traditional frequentist methods. Hence, we implemented the growth model in a Bayesian framework, using minimally-informative priors, in the 'brms' package in R 3.3.0 (*81*). We assessed model convergence using R-hat statistics for the posterior distribution of each parameter, and model fit by comparing the distribution of the training data to the distribution of the mean posterior predictions of those observations, across the entire dataset and by each site individually. For each site, we compared model fitted to observed values by calculating the standard deviation, Pearson's *r*, and root mean squared error of the model's mean posterior predictions, visualized in a Taylor diagram (Fig. S5). In addition, we plotted these site-level fitted values and their 95% credible intervals as growth time series for visual comparison to observed values (Fig. S6).

Near-past predictions

To evaluate whether observed growth better matched predictions derived from species-wide or population-specific climate responses, we predicted growth at each site in response to observed climatic conditions after the onset of warming. These predictions were made based on species-wide versus population-specific responses separately. Specifically, for species-wide responses, observed 30-year rolling mean climate normals in the post-warming period were entered into the model *CN* terms, while setting all other climate effects at zero, such that the predicted effect of changing climate depended upon the estimated values of $\boldsymbol{\beta_{2i}}$. For population-specific responses, observed post-warming seasonal climate values were substituted into *TA* and *PA* terms, while keeping all other climate effects at zero, such that the predicted effect of changing climate depended upon the estimated values of $\boldsymbol{\beta_{3j}}$, $\boldsymbol{\beta_{4j}}$, $\boldsymbol{\gamma_{2j}}$, and $\boldsymbol{\gamma_{3j}}$. In these post-warming predictions, we used observed tree sizes $BA_{t,s,y}$ so that model-predicted growth could be directly compared against observed growth. We used Pearson's correlation coefficient between the observed and predicted growth series for each tree in the dataset to quantify their correspondence. For species-wide predictions, we converted observed growth series to 30-year rolling means to match the scale of variability in the predicted series.

Future projections

We then used the growth model to project future tree growth using climate projections from the CMIP6 ensemble dataset for future scenarios SSP1-2.6, SSP2-4.5, and SSP5-8.5 (Eyring et al. 2016) downscaled and extracted using ClimateNA 7.3.0 (*82*). We aggregated monthly climate projections to recreate the same mean, annual, and seasonal climate variables used in fitting the growth model (Equation 1). We used these future climate data to project growth through the end of the 21st century for each tree by forcing the model with the species-wide versus population-level responses to climate variation separately, as described above. To make species-wide growth projections, we entered future 30-year mean annual temperature and precipitation projections into the *CN* term in our growth model, while setting the effects of annual climate variables *TA* and *PA* to zero. For population-specific projections, we set the effects of *CN* model terms to zero, and entered in projected future *TA* and *PA* time series. Both projection types were made with all modeled random effects, with tree size *BA* set to the mean observed value in the model fitting period. All model predictions were made using 2000 posterior draws of model parameters, which we summarized with mean posterior predictions and 95% credible intervals.

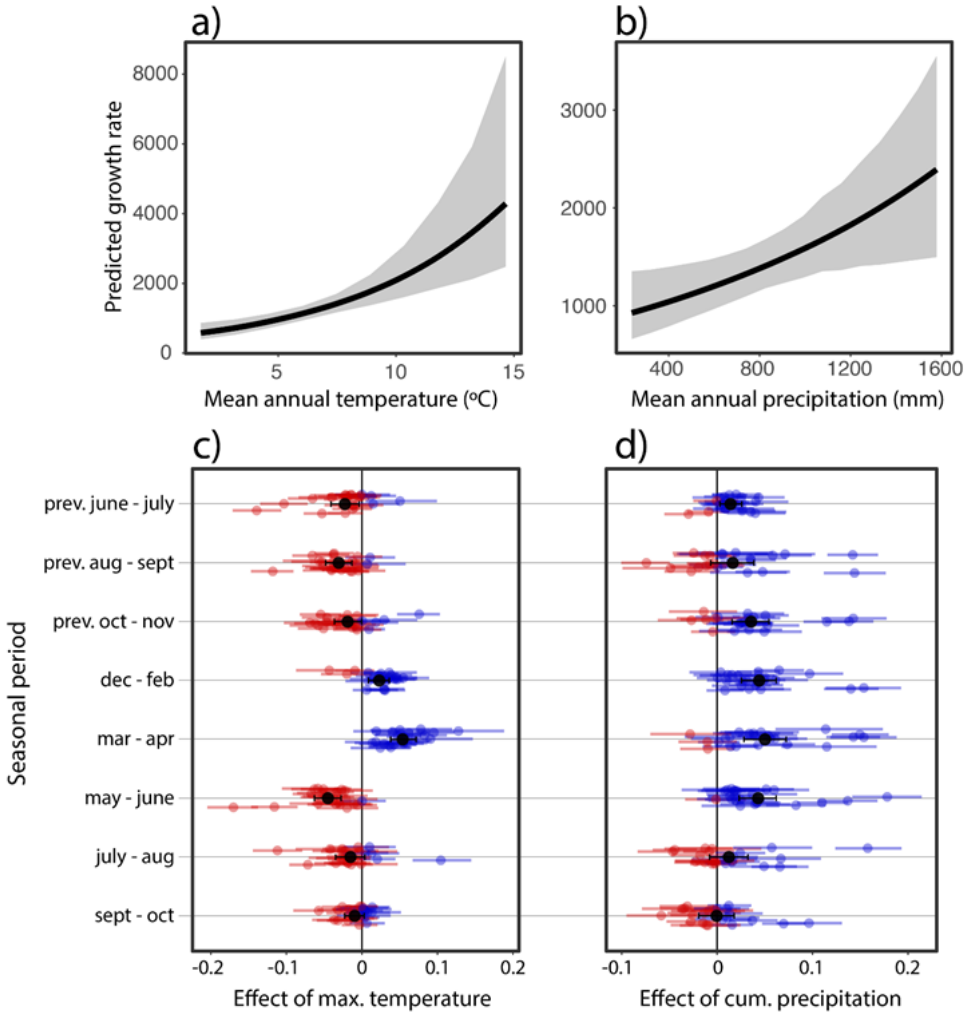

Figure S1. Modeled effects of climate normals and seasonal climate on tree growth. Panels (a) and (b) show the mean estimated marginal effects (black line) and 95% credible intervals (gray shading) of mean annual temperature (a) and mean annual precipitation (b) on basal area increment, corresponding with species-wide growth responses to climate. Panels (c) and (d) show the effects of maximum temperature (c) and cumulative precipitation (d) in each of eight annual seasonal periods (y-axes) ranging from the previous year's growing season through the end of the current year. Effects shown (x-axes) are population-specific mean posterior coefficient estimates (points) and 95% credible intervals (lines). Black dots and bars indicate fixed effect estimates, whereas colored dots and lines indicate population-level random effects, with red indicating a negative mean posterior estimate, and blue indicating a positive mean estimate.

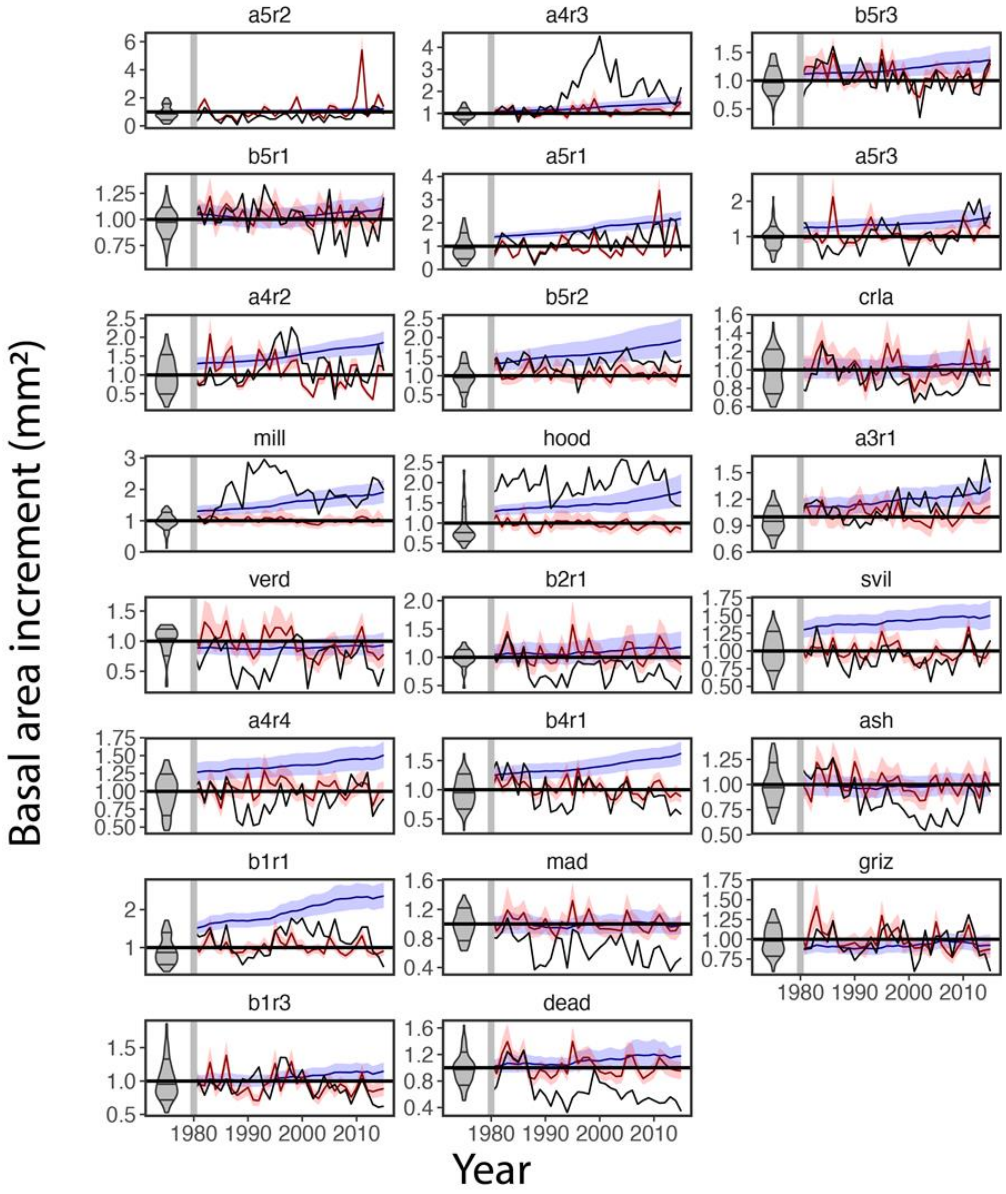

Figure S2. Comparisons of observed post-warming (1980-2015) growth to species-wide and population-specific growth predictions for each study site. For each site (panels), growth is shown relative to pre-1980 mean growth (y axes), with black lines showing observed mean growth. Blue lines and shading indicate species-wide predictions and 95% credible intervals, whereas red lines and shading show the same for population-specific predictions. Gray density plots on the left of each panel show the distribution of relative growth rates in the pre-warming period used to train the growth model. Sites are arranged in order of increasing mean growth rate from top left to bottom right. Figure 2B in the main text shows these results summarized across all sites.

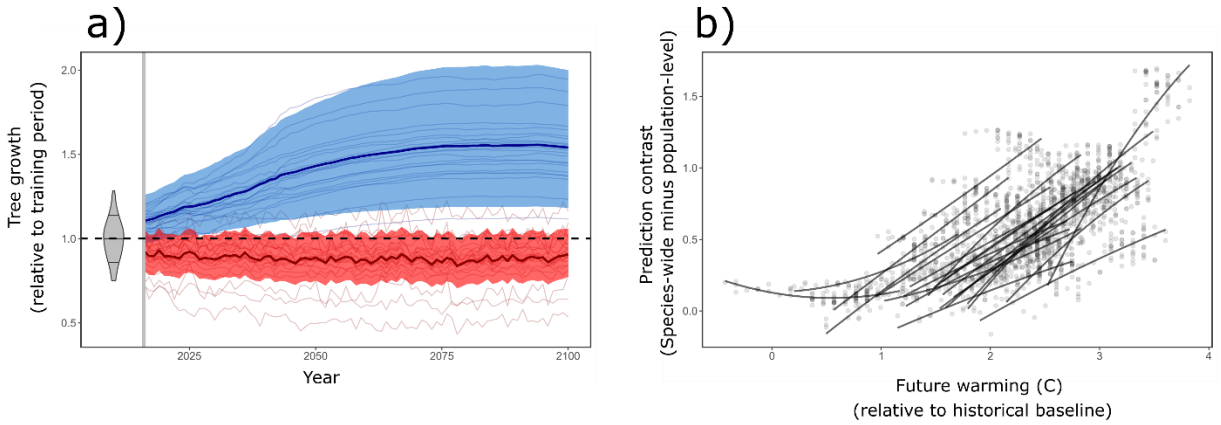

Figure S3. Future growth projections for the CMIP6 SSP1-2.6 climate scenario. Panels (a) and (b) correspond to main text Figure 2D and Figure 2E, respectively. Panel (a) shows divergence between species-wide (blue) and population-level (red) growth predictions under the SSP1-2.6 scenario. Heavy lines and shading indicate mean posterior predictions and 95% credible intervals across all sites, respectively; light lines indicate mean posterior predictions for each site. Vertical gray line indicates the beginning of the future prediction time period (2015-2100), and gray density plot indicates the distribution of mean observed growth across all sites in the model-fitting period (1900-1982). Panel (b) shows contrasts between species-wide and population-level predictions, as a function of projected future warming at each site (black points and lines).

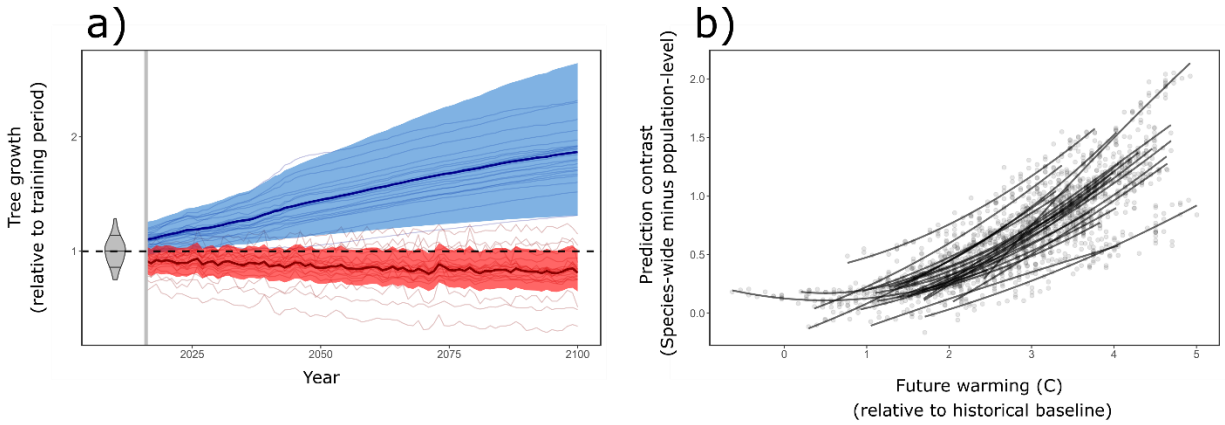

Figure S4. Future growth projections for the CMIP6 SSP2-4.5 climate scenario. Panels (a) and (b) correspond to main text Figure 2D and Figure 2E, respectively. Panel (a) shows divergence between species-wide (blue) and population-level (red) growth predictions under the SSP2-4.5 scenario. Heavy lines and shading indicate mean posterior predictions and 95% credible intervals across all sites, respectively; light lines indicate mean posterior predictions for each site. Vertical gray line indicates the beginning of the future prediction time period (2015-2100), and gray density plot indicates the distribution of mean observed growth across all sites in the model-fitting period (1900-1982). Panel (b) shows contrasts between species-wide and population-level predictions, as a function of projected future warming at each site (black points and lines).

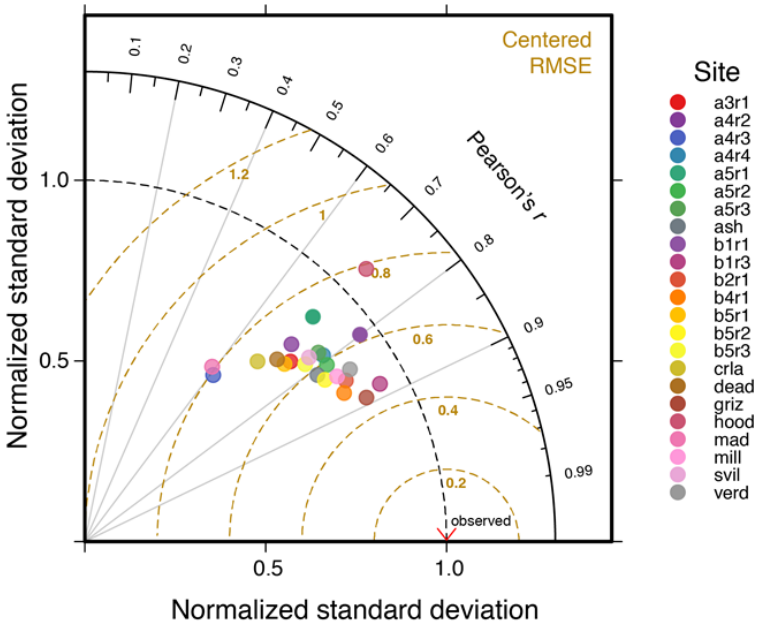

Figure S5. Taylor diagram showing how model fit varied between sites. Each colored point shows how fitted values from our growth model compared to observed growth, according to the normalized standard deviation (x and y axes), Pearson's r (radial axis), and the centered root means squared error (distance from observed data point). The red chevron on the x-axis indicates the observed data (normalized standard deviation = 1; Pearson's r = 1, RMSE = 0). Sites closer to the observed data have a better model fit than those further from the observed data. Site names are solely unique identifiers.

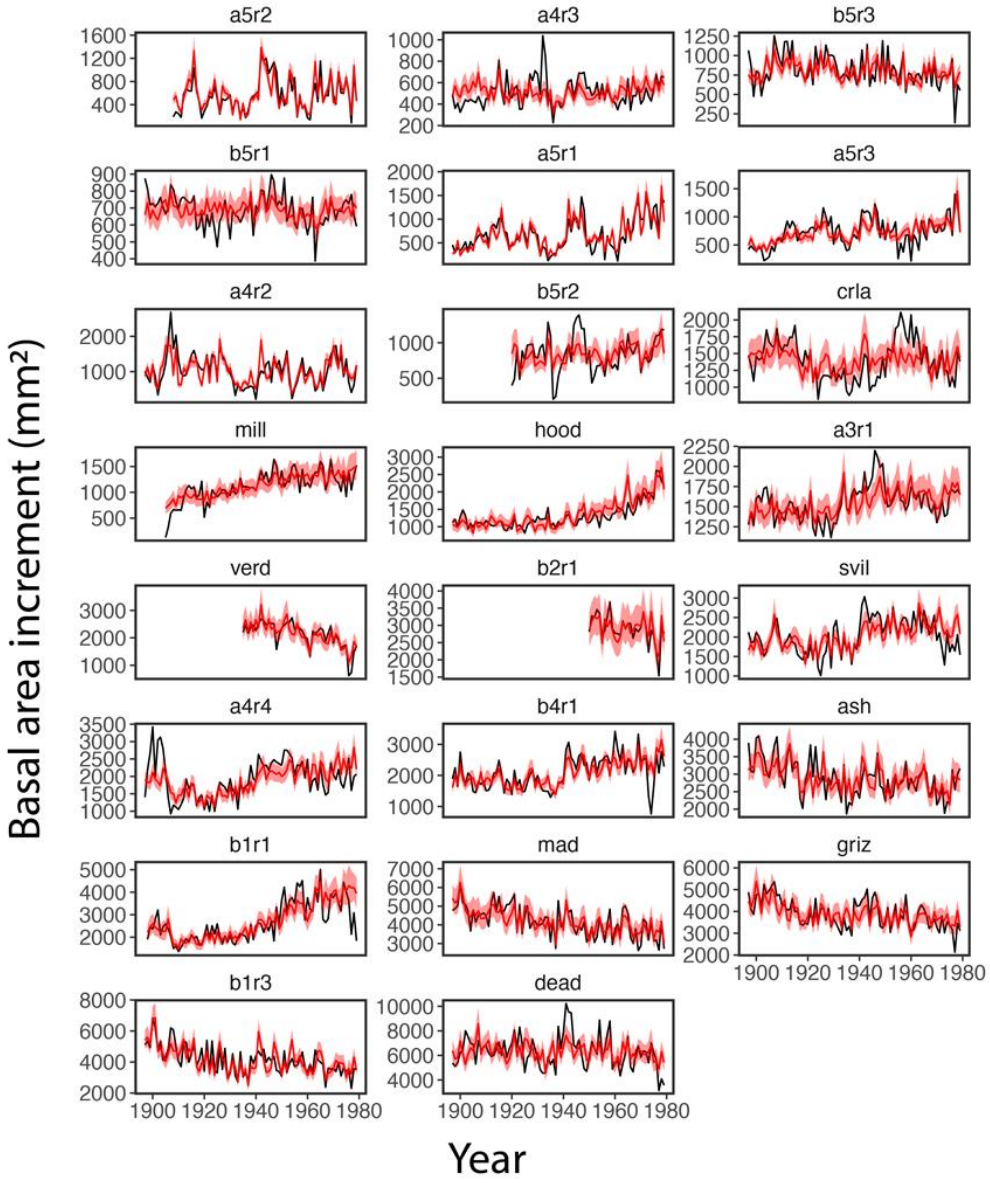

Figure S6. Observed versus modeled growth chronologies in the pre-warming period for each study site. For each site (panels), the black line shows mean annual growth (basal area increment) across all trees in a site. The red line shows the mean posterior prediction from our growth model across all trees in a site, with red shading indicating the 95% credible interval. Sites are arranged in order of increasing mean growth rate from top left to bottom right.

Site ID	State	Longitude	Latitude	Elevation	Series	Rings	Mean Annual Temp		Mean Annual Precip		Mean BAI
							1900-1980	1980-2015	1900-1980	1980-2015	
b1r1	CA	-120.3039	38.1102	2224	8	876	13.8	14.4	983.0	999.1	3403.2
b1r3	CA	-122.8272	40.1412	5828	16	1884	8.5	9.3	1113.5	1163.6	4910.1
b2r1	CA	-120.8742	39.9946	5209	20	1320	9.0	10.1	1026.0	1008.9	2156.7
dead	CA	-120.6913	39.0774	3858	13	1456	12.8	13.8	1335.1	1379.3	6597.7
griz	CA	-119.4119	37.4094	5651	16	1920	9.2	9.7	1153.5	1088.5	4161.0
mad	CA	-123.3587	40.1205	2745	8	952	11.7	12.5	1418.6	1435.5	4114.0
svil	CA	-120.4413	39.6407	5071	20	2395	7.6	8.4	642.5	633.8	2245.9
verd	CA	-120.0670	39.5017	6631	12	972	6.0	7.1	637.5	651.1	1996.0
a4r2	CO	-105.3138	40.1513	6439	21	1959	9.0	9.8	473.4	510.3	1118.7
b5r1	CO	-105.5515	39.6179	9708	21	2467	3.0	3.2	550.4	595.3	836.2
b5r3	CO	-107.0006	39.9073	8525	23	2127	3.7	4.5	487.1	547.7	829.6
a4r4	ID	-116.1189	43.7379	6011	16	1678	6.0	6.4	567.8	602.2	2290.1
b4r1	ID	-116.1303	45.6305	4776	20	2325	6.6	7.1	619.4	630.1	2521.6
a5r1	MT	-105.6563	46.3705	3005	15	1678	6.9	7.6	346.7	352.0	859.2
a5r2	MT	-105.1268	46.8771	2560	21	1850	6.1	6.9	317.7	325.6	603.6
a5r3	MT	-107.8717	47.0979	2987	13	1297	7.5	8.3	313.3	335.6	867.0
b5r2	MT	-109.7412	45.2385	6964	12	847	3.6	4.3	621.7	653.9	1302.0
hood	MT	-114.9938	47.0154	4980	6	647	4.7	5.2	1541.8	1348.2	1924.8
ash	OR	-122.7223	42.0532	5547	15	1716	7.9	8.4	1053.7	1052.8	3139.8
crla	OR	-121.9542	42.8893	5440	6	720	5.5	6.0	1061.4	1086.4	1677.6
mill	OR	-121.7177	44.2390	5024	4	433	5.2	5.7	962.4	1069.3	1846.5
a4r3	SD	-103.6441	44.1446	5652	13	1141	5.2	5.4	519.5	569.7	772.1
a3r1	WA	-120.8097	47.8186	2400	20	2400	6.8	7.4	1069.5	1075.2	1928.6

Table S1 (preceding page). Study site locations and characteristics, including elevation (feet above sea level), number of growth time series ('Series'), number of individual growth rings ('Rings'), mean annual temperature (degrees Celsius) and precipitation (mm) in pre- and post-warming periods, and mean growth rate (basal area increment, mm^2).